ARTICLE
Journal of Cellular Biochemistry 112:1206–1218 (2011)

Journal of Cellular Biochemistry

Isolation and Characterization of Mesenchymal Stem Cells From Human Umbilical Cord Blood: Reevaluation of Critical Factors for Successful Isolation and High Ability to Proliferate and Differentiate to Chondrocytes as Compared to Mesenchymal Stem Cells From Bone Marrow and Adipose Tissue

Xiaohong Zhang,[1] Masako Hirai,[1] Susana Cantero,[1] Rodica Ciubotariu,[2] Ludy Dobrila,[2] Allen Hirsh,[4] Koichi Igura,[4] Hitoshi Satoh,[5] Izuru Yokomi,[6] Toshihide Nishimura,[7] Satoru Yamaguchi,[9] Kotaro Yoshimura,[9] Pablo Rubinstein,[2] and Tsuneo A. Takahashi[1*]

[1]*Cell Therapy Research and Development Laboratory, New York Blood Center, New York, New York*

[2]*National Cord Blood Program, New York Blood Center, New York, New York*

[3]*Cryobiophysica, Inc., Silver Spring, Maryland*

[4]*Department of Regulatory Science, Center for iPS Cell Research and Application, Kyoto University, Kyoto, Japan*

[5]*Laboratory of Tumor Cell Biology, Department of Medical Genome Sciences, Graduate School of Frontier Sciences, The University of Tokyo, Tokyo, Japan*

[6]*Department of Pharmacology, School of Medicine, St. Marianna University, Kawasaki, Japan*

[7]*Department of Immunology, Graduate School of Medical and Dental Sciences, Kagoshima University, Kagoshima, Japan*

[8]*Yamaguchi Hospital, Funabashi, Chiba, Japan*

[9]*Department of Plastic Surgery, The University of Tokyo, School of Medicine, Tokyo, Japan*

ABSTRACT

Human umbilical cord blood (CB) is a potential source for mesenchymal stem cells (MSC) capable of forming specific tissues, for example, bone, cartilage, or muscle. However, difficulty isolating MSC from CB (CB-MSC) has impeded their clinical application. Using more than 450 CB units donated to two public CB banks, we found that successful cell recovery fits a hyper-exponential function of time since birth with very high fidelity. Additionally, significant improvement in the isolation of CB-MSC was achieved by selecting cord blood units having a volume $\geq$90 ml and time $\leq$2 h after donor's birth. This resulted in 90% success in isolation of CB-MSC by density gradient purification and without a requirement for immunoaffinity methods as previously reported. Using MSC isolated from bone marrow (BM-MSC) and adipose tissue

Author Contributions: X.Z. and T.T. designed research; X.Z., M.H., S.C., K.I., and T.T. performed research; R.C. and S.Y. were responsible for cord blood collection; A.H. performed statistical analysis; H.S. and I.Y. performed karyotype analysis; T.N. performed the immunosuppressive study; K.Y. was responsible for adipose tissue collection; L.D. provided advice on cord blood processing; P.R. advised on the manuscript: and X.Z. and T.T. wrote the paper.

Conflict-of-interest disclosure: The authors declare no competing financial interests.

Additional Supporting Information may be found in the online version of this article.

Grant sponsor: The Japanese Ministry of Health, Labor and Welfare; Grant number: HP-D14, H17365022; Grant sponsor: The Japanese Ministry of Education, Culture, Sports, Science and Technology; Grant number: 16390429. Xiaohong Zhang, Masako Hirai, Tsuneo A. Takahashi's former address is Division of Cell Processing, Facility of Cell Processing and Cryopreservation, Tokyo Cord Blood Bank, The Institute of Medical Science, The University of Tokyo 4-6-1, Shirokanedai, Minato-ku Tokyo 108-8639, Japan.

*Correspondence to: Tsuneo A. Takahashi, DSc, Cell Therapy Research and Development Laboratory, New York Blood Center, 310E. 67th Street, New York, NY 10065. E-mail: ttakahashi@nybloodcenter.org
ttakahashi@frontier.kyoto-u.ac.jp

Received 11 January 2011; Accepted 19 January 2011 • DOI 10.1002/jcb.23042 • © 2011 Wiley-Liss, Inc.
Published online 10 February 2011 in Wiley Online Library (wileyonlinelibrary.com).

(AT-MSC) as reference controls, we observed that CB-MSC exhibited a higher proliferation rate and expanded to the order of the 1×10^9 cells required for cell therapies. CB-MSC showed karyotype stability after prolonged expansion. Functionally, CB-MSC could be more readily induced to differentiate into chondrocytes than could BM-MSC and AT-MSC. CB-MSC showed immunosuppressive activity equal to that of BM-MSC and AT-MSC. Collectively, our data indicate that viable CB-MSC could be obtained consistently and that CB should be reconsidered as a practical source of MSC for cell therapy and regenerative medicine using the well established CB banking system. J. Cell. Biochem. 112: 1206–1218, 2011.

KEY WORDS: HUMAN UMBILICAL CORD BLOOD; MESENCHYMAL STEM CELLS; CHONDROGENESIS; DIFFERENTIATION; CELLULAR PROLIFERATION

Mesenchymal stem cells (MSC) have been studied extensively because of their high potential for multi-lineage differentiation and proliferation, characteristics that make the cells useful for therapeutic purposes [Pittenger et al., 1999; Caplan, 2007; Prockop, 2009; Salem and Thiemermann, 2010]. Clinical studies to date have employed MSC isolated from bone marrow derived MSC (BM-MSC) and adipose tissue derived MSC (AT-MSC) [NIH, Clinical Trials, http://www.clinicaltrials.gov/ct2/search]. However, the use of BM-MSC and AT-MSC has disadvantages, including the necessity of invasive harvest of bone marrow (BM) and adipose tissue (AT) from patients or donors. Thus, alternate sources of MSC have been intensively sought, including cells from human placental tissues, that is, amnion, microvillus, Wharton's jelly and umbilical cord perivascular cells [Igura et al., 2004; Sarugaser et al., 2005; Zhang et al., 2006; Parolini et al., 2008; Troyer and Weiss, 2008]. However these tissues require complex procedures for cell isolation including enzymatic digestion or prolonged culture when using the tissue explants method.

It is well known that there are MSC in human umbilical cord blood (CB-MSC), but clinical application of these cells has not yet been achieved because of their low frequency in cord blood (CB) and the inconsistency of successful isolation of them. In this study we reexamined factors for successful isolation of CB-MSC and the potential of CB to serve as a source of MSC. CB has several advantages, including more than a decade of use in reconstitution of hematopoietic tissue to treat hematological disorders and other diseases [Wagner and Gluckman, 2010]. Moreover, CB banking systems have been developed worldwide meeting technical requirements for clinical grade cellular products [Rubinstein et al., 1995; Rubinstein, 2009; Garcia, 2010]. In 1994, Ye et al. first reported evidence of mesenchymal-like cells in CB that adhered to plastic and supported long-term hematopoietic stem cell growth, even though the cells were not described specifically as MSC [Ye et al., 1994]. Erices et al. [2000] concluded that the adhesive cells in CB were MSC in 2000, and since then many laboratories have reported the isolation, proliferation and differentiation capabilities of CB derived MSC [Bieback et al., 2004; Lee et al., 2004; Yu et al., 2004; Kern et al., 2006; Secco et al., 2008; Zeddou et al., 2010]. Problems in isolating CB-MSC are likely the main reason in limiting research of their potential clinical use [Flynn et al., 2007; Secco et al., 2008; Zeddou et al., 2010]. Our first objective was to identify key parameters required to isolate MSC from CB consistently. Our second objective was to characterize the biological properties of CB-MSC as compared to BM-MSC and AT-MSC, and with respect to several factors related to their practical utility as a tissue source for therapeutic MSC. These include proliferation kinetics, chromosome stability, gene expression and differentiation capabilities to osteoblast, adipocyte, and chondrocyte lineages in vitro. Clinical trials have demonstrated that the infusion of BM-MSC and AT-MSC could ameliorate severe acute graft versus host disease (aGVHD) [Le Blanc et al., 2008; Prasad et al., 2010]. Therefore, we also tested whether CB-MSC have the same immunosuppressive effect as BM-MSC and AT-MSC in vitro. Other MSC-like cells have also been described in CB, and are referred to as unrestricted somatic stem cells (USSC), based on their ability to differentiate into three-germ layers, and which have been studied extensively as cells distinct from CB-MSC [Kögler et al., 2004, 2005; Kluth et al., 2010]. We examined the expression of DLK-1 (delta-like-1, a pre-adipocyte factor) [Sul, 2009] as a way to distinguish CB-MSC from USSC in CB. Results obtained in this study indicate that CB-MSC can be a potentially practical source of cells for cell therapy and regenerative medicine.

MATERIALS AND METHODS

CORD BLOOD COLLECTION

CB was collected from umbilical cord after the delivery of placenta (ex utero) at the New York Presbyterian Hospital (New York) and other hospitals in the National Cord Blood Program (NCBP) of New York Blood Center (NYBC), or while in utero at the Yamaguchi Hospital (Funabashi, Japan). Maternal consent to collect and donate CB to the NCBP was obtained under procedures approved by the NYBC Internal Review Board (IRB) as well as the IRB of each participating hospitals. The study was approved by the IRB of the Institute of Medical Science, the University of Tokyo (IMSUT). CB units were collected in bags with anticoagulant (citrate phosphate dextrose) and were stored at 22°C until isolation of mononuclear cells (MNC).

ISOLATION OF CB-MNC AND COLONY FORMING UNIT FIBROBLAST ASSAY

In our standard method, whole CB was loaded on Ficoll-Paque solution (Ficoll-Paque™ Plus, GE Healthcare, Bio-Sciences, AB). After density gradient centrifugation at 400*g* for 30 min at room temperature, MNC were removed from the interphase and washed twice with phosphate-buffered saline (PBS, Invitrogen). Cell count was performed using automated cell analyzers (XE-2100, Sysmex; Hmx Hemocytometer, Beckman Coulter).

Colony-forming unit fibroblast (CFU-F) assay was performed as follows. MNC were placed in culture at a density of $1–2 \times 10^6/cm^2$ into culture dishes (100-mm diameter, BD Falcon) in Dulbecco's modified Eagle's medium (DMEM: low glucose, Sigma–Aldrich) supplemented with 20% fetal bovine serum (FBS) (Japan BioSerum, Invitrogen Gibco) and incubated at 37°C in 5% CO_2 in air

atmosphere. Dexamethasone (10^{-7} M) (Sigma–Aldrich) was added in the primary culture medium for a week to reduce the adherence of monocytes in the plates. After culture for 1 week, non-adherent cells were removed with medium change, and remaining cells were fed weekly with culture medium without dexamethasone. The colony cells were harvested using 0.25% trypsin/0.5 mM EDTA (Invitrogen). Individual colonies were picked up using cloning cylinders (Millipore). For expansion, the cells were seeded at a density of 1×10^4 cells/cm^2. The medium was changed twice weekly and proliferation curves were obtained by counting cells each week. Single cell cloning culture was performed from clones obtained from primary cultures and expanded cells in 96-well plates. Briefly, MSC single cell clones were generated by limiting dilution at 0.5 cells/well in 96-well microplates containing 120 μl/well of mixed fresh and conditioned medium (1:1.4) [Russell et al., 2010]. Conditioned medium was medium in which CB-MSC had been grown for 48 h. This medium was sterile-filtered (0.2 μm pore size) to remove any suspended cells. Fresh medium (50 μl) was added to each well every 3 days. When the culture reached 80% confluence, the clones were detached and expanded as described above.

MODIFIED METHODS FOR ISOLATION AND CULTURE OF CB-MSC

CB-MSC were isolated and cultured by the following modified methods.

Hydroxyethyl starch sedimentation method. Nucleated cells in CB were separated by the hydroxyethyl starch (HES) method [Rubinstein et al., 1995]. Briefly, 1/5 volume of HES (HESPAN, B. Braun Medical) was added to CB to sediment erythrocytes, and the supernatant was centrifuged at 150*g* for 5 min to concentrate the cells. The cells were washed with PBS twice and nucleated cells were plated on plastic plates and cultured as described in supplementary Methods.

Depletion of hematopoietic cells and immunological cells from MNC. For some studies, hematopoietic cells, lymphocytes, and monocytes were removed from MNC using RosetteSep® human progenitor enrichment cocktail (STEMCELL Technologies). This cocktail contains a combination of monoclonal antibodies which are directed against cell surface antigens in human hematopoietic cells (CD2, CD3, CD14, CD16, CD19, CD24, CD56, CD66b) and glycophorin A.

Collagen and fibronectin coated plates. MNC isolated by Ficoll-Paque gradient centrifugation were plated on collagen type I, or fibronectin pre-coated plates (BD Biosciences) or manually coated with CellStart™ (Invitrogen). Cells were cultured as described above.

Hypoxia culture. Isolated MNC were cultured under hypoxic condition (5% O_2, 5% CO_2, 90% N_2) in a CO_2 incubator (Sanyo Biomedical).

Addition of cytokines for primary culture. Isolated MNC were cultured with DMEM (Sigma–Aldrich) plus 20% FBS (Japan Bioserum and Invitrogen) with IL-3 (10 ng/ml), SCF (10 μg/ml), and FGF-2 (10 ng/ml) (PeproTech) for 2 weeks.

Success or failure of isolating CB-MSC was judged by the appearance of colonies after 4 weeks after plating.

CRYOPRESERVATION

Cryopreservation of CB-MSC and CB-MNC was performed by standard slow cooling rate freezing. For details, see supplementary Methods.

ISOLATION OF MSC FROM AT AND BM

Adipose tissue from healthy donor was obtained from elective liposuction procedure under anesthesia after informed consent was obtained.

Fresh whole BM aspirates were purchased from Veritas Pharmaceutical. For detailed technical information see supplementary Methods.

CUMULATIVE POPULATION DOUBLING LEVEL (PDL)

See supplementary Methods.

SECONDARY COLONY FORMING ABILITY OF PRIMARY CULTURED CB-MSC, BM-MSC, AND AT-MSC

To compare the colony forming ability of CB-MSC, BM-MSC, and AT-MSC, 50, 200, and 1,000 cells from primary culture were seeded on 60-mm-diameter dishes (BD Falcon Bioscience). After 2 weeks of culture, the colonies were stained with Giemsa (Sigma) and those colonies larger than 2 mm in diameter were counted.

FLOW CYTOMETRY ANALYSIS

For technical information see supplementary Methods.

TELOMERASE ACTIVITY AND TELOMERE LENGTH ASSAY

For details, see supplementary Methods.

FLUORESCENCE IN SITU HYBRIDIZATION (FISH) ANALYSIS

FISH analysis was performed by standard procedure. For details see supplementary Methods.

CYTOGENETIC ANALYSIS

For detailed procedure and technical information, see supplementary Methods.

LARGE SCALE EXPANSION OF CB-MSC

For large scale expansion, CB-MSC were first cultured in DMEM containing 20% FBS in 150-cm^2 flasks (BD Falcon) until the number of cells reached $\sim 3 \times 10^7$. For scale-up expansion, cells were transferred into a CellSTACK 5-STACK (3,150 cm^2 cell growth area, Corning) culture chamber. After cells reached 80% of confluence, they were transferred to three 10-STACK (6,300 cm^2 each) culture chambers.

DIFFERENTIATION TO CHONDROCYTES, OSTEOCYTES, AND ADIPOCYTES IN VITRO

Chondrogenic, osteocytic, and adipocytic induction were performed as described previously [Zhang et al., 2006]. For detailed procedures see supplementary Methods.

DETECTION OF DIFFERENTIATION ABILITY IN VITRO

See supplementary Methods.

IN VIVO CHONDROGENESIS AND OSTEOGENESIS OF CB-MSC

Animal studies were approved by the Institutional Animal Committee of the IMSUT. For detailed procedure and technical information, see supplementary Methods.

RT-PCR AND REAL TIME PCR

Human-specific PCR primers used in this study were as follows: Sox9, COL 2A1, Aggrecan, COL10A1, BMP-6, β-actin, BMPR-IA, BMPR-IB, BMPR-II, Smad1, Smad5, Smad8, Sox5, Sox6, Cbfa1, PPAR-γ1, PPAR-γ2, Oct-4, Nanog, alpha-fetoprotein (AFP), fetal liver kinase-1 (FLK-1), neural cell adhesion molecule (NCAM), c-Myc, and DLK-1. For detailed information, see supplementary Methods.

INHIBITORY EFFECTS OF MSC ON PROLIFERATION OF STIMULATED T-LYMPHOCYTE AND BY MIXED LYMPHOCYTE REACTION (MLR)

Peripheral blood was obtained from healthy volunteers after informed consent. For T-cell stimulation assay details see supplementary Methods.

STATISTICS

For statistical analysis, Student's *t*-test was applied unless indicated otherwise. *P* values less than 0.05 were considered to be significant. Further details on statistical analysis of the data are provided in the supplementary Methods.

RESULTS

A total of 467 CB units were obtained in this study (Table S1). The CB units with blood clots and hemolysis detected before or after MNC isolation were removed from the study (11 out of 467 units, corresponding to 2.3%). The remaining 456 units were used in the study. The number of units used in individual assays is indicated below.

MSC COLONIES OBTAINED FROM CB

The mean volume (±SD) of 456 CB units was 63.12 ± 19.47 ml (range, 19.5–171.0 ml) without anticoagulant. There was a reasonable correlation between volume and MNC ($r^2 = 0.522$, Fig. S1). The mean time between collection of CB at the collection facilities and start of processing, that is, loading CB on Ficoll-Paque solution, mixing with HES, or mixing with immunobeads, was 6.4 ± 9.2 h (0.5–53 h, $n = 427$). Using our standard method, CB-MSC colonies were isolated from 165 CB units of 345 units (47.8%) (Table S2). The mean number of MNC per unit after isolation was $2.01 \pm 0.75 \times 10^8$ ($0.80–4.15 \times 10^8$, $n = 210$). The colonies were detected at 13.9 ± 2.8 days (range, 4–19 days, $n = 114$) after plating MNC in the primary culture medium (Fig. 1Aa). The mean number of CB-MSC colonies from the units from a representative subset of harvested units was 3.67 ± 2.68 CFU-F/CB unit (range, 1–17 CFU-F/CB unit, $n = 63$) or 2.10 ± 1.93 CFU-F/10^8 MNC. The mean number of cells obtained from primary culture after 10 days of colony appearance was $16.5 \pm 11.5 \times 10^5$ (range, $1.8–52.8 \times 10^5$, $n = 104$). CB-MSC exhibited a small spindle-shape morphology (Fig. 1Ab), grew rapidly, and expanded for more than 40 PDL (>12 passages) without significant morphological changes or reduction of proliferation rate (Fig. 1B). FISH analysis to identify XY chromosomes in CB-MSC isolated from CB of male neonates produced a mean XY incidence of $98.38 \pm 0.01\%$ ($XX = 0.00 \pm 0.00\%$, $n = 8$) indicating that CB-MSC were of fetal origin.

NON-PROLIFERATIVE FIBROBLAST-LIKE CELLS AND OSTEOCLAST-LIKE CELLS FROM CB

The CB-derived adherent cells after 1 week of culture consisted of at least three morphologically distinct cell types: expandable spindle-shaped fibroblastic cells (CB-MSC), osteoclast-like cells, and non-proliferative fibroblast-like cells (Fig. 1A). The spindle-shaped cells proliferated most rapidly. In contrast, non-proliferative fibroblast-like cells and osteoclast-like cells adhered to the bottom of culture dishes firmly in primary plating, did not proliferate and were stained with ammonium tartrate (Fig. S2A). Surface phenotypes of these adherent cells were different from CB-MSC (Fig. S2B,C).

ISOLATION AND PROLIFERATION OF BM-MSC AND AT-MSC

BM-MSC and AT-MSC appeared at 3–5 days after first plating. MSC could be isolated from 6 of 6 BM samples and 21 of 21 AT samples. All isolated MSC populations from BM and AT displayed a spindle-shaped fibroblastic morphology (Fig. 1A). The proliferation rate of MSC slowed after approximately 10–20 PDL (passage 8–10) (Fig. 1B). When the cells appearing in the primary cultures were plated using different cell densities (50, 200, or 1,000 cells/plate; 60 mm), CB-MSC formed more secondary colonies than AT-MSC (Fig. 1C). In addition, the colonies of CB-MSC contained more cells, as indicated by more intense Giemsa staining.

CRITICAL FACTORS FOR SUCCESSFUL ISOLATION OF CB-MSC

The factor that contributed the most to improving the rate of isolating CB-MSC was the interval between collection of CB and start of cell processing.

Success or failure of isolating CB-MSC in each CB unit by the standard method was plotted on rectangular coordinates of volume and time for analysis (Fig. S3). For determining success of isolating CB-MSC versus time to process irrespective of CB volume harvested, we used the Kolmogorov–Johnson–Mehl–Avrami (KJMA) hyper-exponential decay model of viability common to many nucleation processes [Ben-Naim and Krapivsky, 1996] which we have shown can also be applied to mortality processes [Williams et al., 1992; Hirsh et al., 1994]. Using this equation we obtained a very high fidelity of fit to the survival data for colony forming cells, that is, success of isolation of CB-MSC, from 1 h to just over 37 h, $S = \mathrm{Exp}(-0.46 \times t^{0.31})$ ($r^2 > 0.96$, $n = 272$, Fig. 2A; see details of calculation in legend of Fig. 2).

In contrast to time based analysis irrespective of volume, there was a more modest, but still highly significant, increase in S from increasing volume irrespective of time: $S = 0.0034\,V\,(\mathrm{ml}) + 0.2244$ ($r^2 > 0.85$, $n = 249$, Fig. 2B). When volume was ≥90 ml and time was ≤2 h, the success rate appeared to increase to above 90% (Fig. 2C). However, a χ^2 test of these data indicated that to achieve $P < 0.05$ the sample size at ≥90 ml would have had to be at least 50. Nevertheless, that extremely high success rate is consistent with what one would expect if the trends of the curves of Figure 2A,B

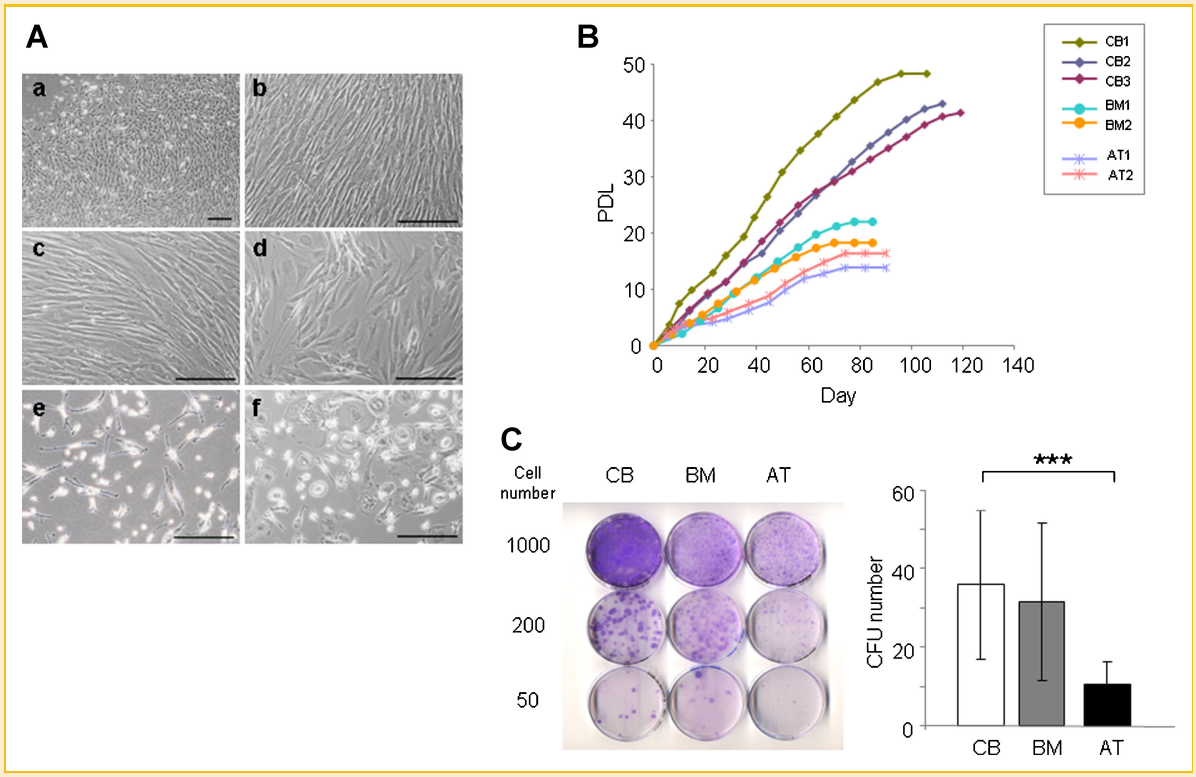

Fig. 1. Morphology, proliferation, and secondary colony formation of CB-MSC, BM-MSC, and AT-MSC. A: Morphology of CB-MSC, BM-MSC, and AT-MSC. a: A colony of CB-MSC appeared 14 days after initial plating, (b) proliferated CB-MSC (first passage), (c) proliferated BM-MSC (first passage), (d) proliferated AT-MSC (first passage), (e) non-proliferative fibroblast-like cells (primary culture), (f) osteoclast-like cells (primary culture). Scale bars: 200 μm. B: Growth curves of CB-MSC, BM-MSC, and AT-MSC. Each line shows the growth curve of isolated MSC from different cell lines. Each mark indicates the day of cell passage. C: Secondary colony formation of primary CB-MSC, BM-MSC, and AT-MSC. Graded numbers (50, 200, and 1,000) CB-MSC, BM-MSC, and AT-MSC cells from primary cultures of three donors were plated in 60-mm culture dishes. After 2 weeks, the colonies were stained by Giemsa and the number of colonies with diameter larger than 2 mm was counted. Left: CB-MSC colonies show stronger Giemsa staining than those from BM-MSC and AT-MSC. Right: Number of colonies obtained when 200 cells were plated. $^{***}P < 0.001$.

were in effect simultaneously. On this basis we feel that this data points to a very significant positive effect of a combination of short times and large volumes.

There was no difference in success rates for samples collected at two different locations, which would reflect background differences of races or different CB collection methods (in utero vs. ex utero collection). There was also no correlation based on differences in gender ($P = 0.084$, Table S3).

No statistically significant differences in the success rate of isolating CB-MSC were observed using different isolation methods or culture conditions (Table S2). There was no time difference to prepare samples among standard and modified methods.

IMMUNOPHENOTYPE OF MSC

Surface phenotypes of CB-MSC, BM-MSC, and AT-MSC were strongly positive for mesenchymal progenitor/stem cell related antigens such as CD29, CD44, CD73, CD90, CD105, CD166, and HLA-ABC and were negative for CD14, CD31, CD45, CD271, HLA-DR, and NG2. The hematopoietic progenitor and endothelial related antigen, CD34 was not expressed on CB-MSC or BM-MSC, but was expressed on AT-MSC (mean percent positive cells: $28.0 \pm 24.7\%$, range, 4.0–66.5%, $n = 10$). All positive surface markers were observed at high percentage of cell populations in all CB-MSC (Fig. 3A).

Regarding to CD146 expression on CB-MSC, a typical surface antigen appearing on perivasucular cells and pericytes, a wide range of differences was observed in the 20 CB units tested (range 3.5–98.4%; Fig. 3B). No significant difference in CD146 expression was observed in CB-MSC at different passages from the same unit (Fig. S4A).

However, when we isolated different clones from one unit and expanded them separately, we sometimes observed different percentages of CD146 expression between them. There were no CD146 expression differences between single cell clones and the clone from which they were isolated (Fig. S4B,C). On the other hand, CD146 expression in BM-MSC was as high as 65–90%, whereas CD146 was not expressed on AT-MSC. Human umbilical vein endothelial cells (HUVEC) were used as positive control (ATCC).

LARGE SCALE EXPANSION OF CB-MSC

CB-MSC (5 passages) were expanded to $2.93 \pm 0.12 \times 10^7$ cells ($2.80–3.00 \times 10^7$, $n = 3$) in 150-cm^2 flasks for 7 days. Cells were then transferred to a 5-STACK culture chamber until the cell number reached approximately 2.5×10^8 ($2.59 \pm 1.27 \times 10^8$, range, $1.27–3.80 \times 10^8$). From the expanded CB-MSC, 1.58×10^8 cells were continuously cultured in three 10-STACK units. After culture for 13 days, 1.02×10^9 cells were harvested (Fig. 3C). The expanded

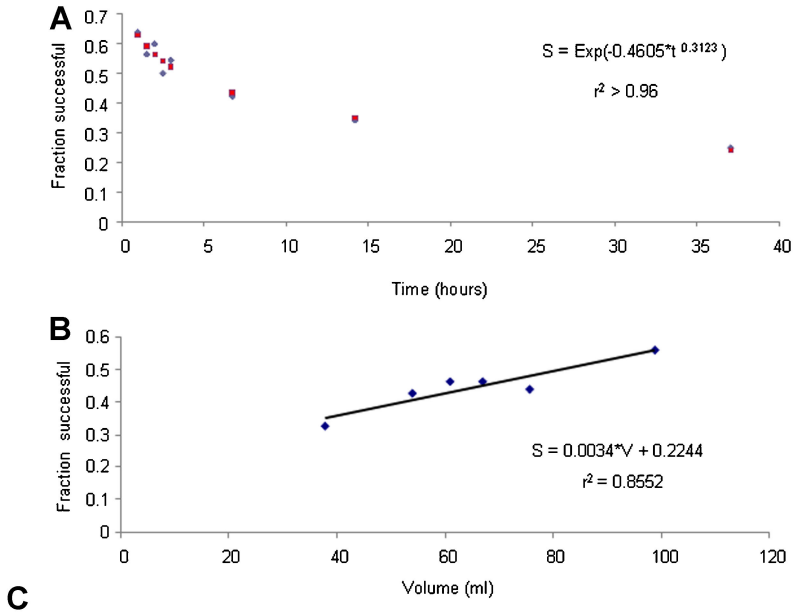

C

Volume (V) and Time (T)		Processed units, no.	MSC isolated units, no.	Success rate, %	Volume[a], ml	Time[a], hours
All volume	0 < T ≤ 2 hours	163	99	60.7	62.34 ± 17.02	1.4 ± 0.4
	2 < T ≤ 6 hours	59	31	52.5	65.64 ± 22.97	3.7 ± 1.1
	6 < T ≤ 20 hours	62	18	29.0	65.09 ± 23.93	13.6 ± 4.3
≤ 2 hours	V < 60 ml	88	48	54.5	50.72 ± 6.81	1.4 ± 0.4
	60 ≤ V < 90 ml	64	41	64.1	70.80 ± 7.21	1.4 ± 0.4
	V ≥ 90 ml	11	10	90.9	106.14 ± 14.47	1.4 ± 0.5

Fig. 2. Critical factors for successful isolation of CB-MSC. A: Effect of time on successful isolation of CB-MSC. Two critical factors contributing to the success rate of isolating CB-MSC were: interval between collection of CB and processing of cells, and CB volume. For colony formation versus time irrespective of volume we used as an initial approach the Kolmogorov–Johnson–Mehl–Avrami (KJMA) hyper-exponential decay model of viability common to many nucleation and mortality processes. This relation has the form: $S = S_0\exp(-kt^{\alpha})$. Here S is fraction of samples forming colonies at time t, S_0 is fraction successful at zero time, taken as 1 with k and α fitting constants. We obtained a very high fidelity fit of the survival data of Ficoll-Paque isolated cells from 1 h to just over 37 h ($r^2 > 0.96$, $n = 272$). Since $(dS/dt) = (-\alpha k/t^{(1-\alpha)})S$, the coefficient of S, instead of being a constant as in classical exponential decay, is monotonically decreasing. Thus the rate of loss of cells slows with time. Blue points mean experimental colony forming fraction at each time, red points are KJMA. Data were grouped in blocks of as close to 30 as possible and each block averaged, except for the large block of data at $t \leq 2$ h. For these data time of isolation is exact. Detailed data are shown in supplemental Figure 3. B: Effect of volume on successful isolation of CB-MSC. Data were grouped in blocks of approximately 40 and each block was averaged. In contrast to time based analysis irrespective of volume, there was a more modest increase in success from increasing volume irrespective of time. C: Effect of time and volume on success rate of isolating CB-MSC. [a]Mean ± SD.

cells showed chondrogenic and osteoblastic differentiation (Fig. 3D). However, the size of chondrogenic pellets of expanded CB-MSC was about 50% smaller than those made by the same CB-MSC line before transfer to the 5-STACK culture chamber (diameter of pellets pre-transfer 2.5 ± 0.6 mm, post-transfer 1.3 ± 0.2 mm, n = 3, $P < 0.05$). These cells were continuously cultured through more than five passages and proliferated to 25 PDL (Fig. 3C).

CRYOPRESERVATION OF CB-MSC AND ISOLATION OF CB-MSC FROM CRYOPRESERVED MNC

After proliferation, CB-MSC were cryopreserved using a slow freezing method without significant loss of cells. Viability tested by trypan blue dye exclusion assay and cell recovery was 95.7 ± 0.7% and 95.5 ± 2.5% (n = 6), respectively. From the cryopreserved MNC isolated from seven CB units (mean volume 67.40 ± 9.91 ml, mean time from harvest to processing 1.6 ± 0.7 h), CB-MSC were obtained from four samples (success rate 57.1%), the success rate was in the range that we obtained from a much larger group of fresh and non-frozen samples.

CYTOGENETIC STABILITY OF CB-MSC LINES

The CB-MSC line analyzed in this study possessed largely normal karyotypes in spite of massive expansion (Fig. 3E and Fig. S5). A clonal expansion of cells with an unbalanced chromosome translocation was detected in CB5, but the rate was low (2/73; 2.7%). Besides, 2.6% (2/76) of cells with aneuploid appeared in CB1 at passage 16 and the cells undergoing endoreduplication were detected in CB1, CB2, and CB5.

TELOMERASE ACTIVITY AND TELOMERE LENGTH IN CB-MSC, BM-MSC, AND AT-MSC

No telomerase activity was detected in CB-MSC, BM-MSC, and AT-MSC from primary cultures or from expanded cultures (Fig. S6A). Greatest telomere length was found in CB-MSC (11.73 ± 0.32 kbp,

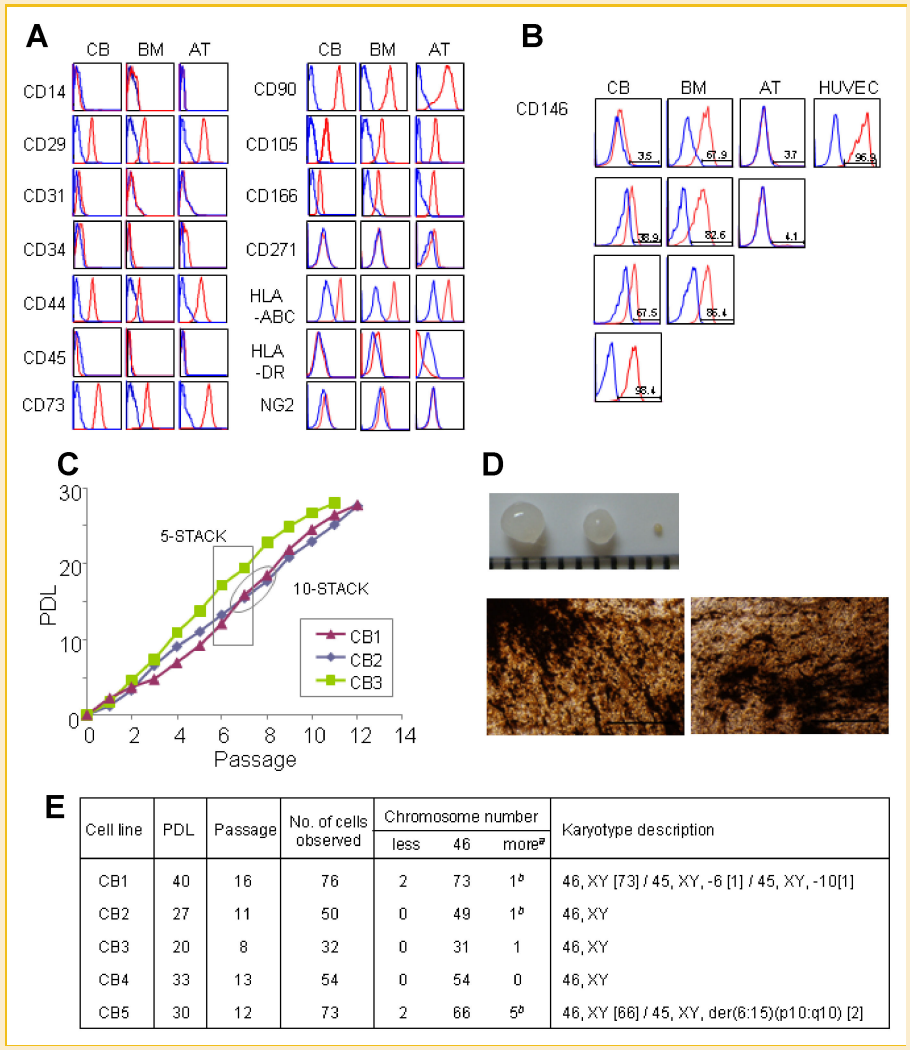

E

Cell line	PDL	Passage	No. of cells observed	Chromosome number			Karyotype description
				less	46	more[a]	
CB1	40	16	76	2	73	1[b]	46, XY [73] / 45, XY, -6 [1] / 45, XY, -10[1]
CB2	27	11	50	0	49	1[b]	46, XY
CB3	20	8	32	0	31	1	46, XY
CB4	33	13	54	0	54	0	46, XY
CB5	30	12	73	2	66	5[b]	46, XY [66] / 45, XY, der(6:15)(p10:q10) [2]

Fig. 3. Immunophenotype of CB-MSC, BM-MSC, AT-MSC, and large scale expansion of CB-MSC. A: Surface immunophenotype of CB-MSC, BM-MSC, and AT-MSC. Blue curves show isotype controls and red curves show tested samples. Each histogram is a representative result of 24 CB-MSC lines, 4 BM-MSC lines, and 10 AT-MSC lines. B: CD146 expression. Histograms showing CD146 expression in representative samples of CB-MSC, BM-MSC, and AT-MSC cell lines. CB-MSC showed different range of positivity for CD146 antigen. BM-MSC expressed high percentage of CD146 positivity, whereas AT-MSC were negative for CD146 antigen. Red line: CD146; blue line: isotype control. C: Large scale expansion of CB-MSC. Square mark: 5-CellSTACK stage; oval mark: 10-CellSTACK stage. D: Differentiation abilities of large-scale expanded CB-MSC. Top: Pellets generated from CB-MSC before and after large scale expansion. Left to right: a pellet generated from CB-MSC after six passages, a pellet generated from CB-MSC after expansion in 5-STACK (seven passages), and a pellet of six passages cultured without BMP-2 and TGF-β. Scale bar, 1 mm. Bottom: Osteogenic differentiation demonstrated by deposition of mineralized matrix as detected by von Kossa staining. Before large scale expansion (six passages) (left) and after large scale expansion in 5-STACK (seven passages) (right). Scale bars, 200 μm. E: Stability of karyotypes of expanded CB-MSC. Karyotype analysis of 5 CB-MSC cell lines. [a]All metaphases observed were tetraploid cells. [b]Metaphases undergoing endoreduplication were recorded (in each CB-MSC line).

four passages, n = 3) compared to BM-MSC (9.60 ± 0.86 kbp, four passages, n = 3, $P < 0.05$) or AT-MSC (10.33 ± 0.68 kbp, four passages, n = 3, $P < 0.05$; Fig. S6B).

OSTEOGENIC, CHONDROGENIC, AND ADIPOGENIC DIFFERENTIATION OF CB-MSC, BM-MSC, AND AT-MSC IN VITRO

After 3 weeks of osteogenic induction, all CB-MSC (n = 45), BM-MSC (n = 6), and AT-MSC (n = 21) showed osteogenic phenotypes detected by alkaline phosphatase staining (data not shown) and von Kossa staining (Fig. 4A).

In CB-MSC induced to osteogenesis, significantly higher ALP activities were detected in the induced cells than in cells from the control culture (n = 6, $P < 0.001$; Fig. S7). The levels of osteocalcin and calcium were also significantly higher in the cell layer after 2 weeks of inductive culture compared to control cells (n = 6, $P < 0.05$).

After 3-week culture with TGF-β3 and BMP-2, a significant increase in pellet size was found in 100% of CB-MSC (45 of 45) and BM-MSC (6 of 6). In contrast, the pellets obtained from AT-MSC (21 of 21) were small (Fig. 4B). Pellets from CB-MSC were heavier than BM-MSC ($P < 0.05$) and AT-MSC ($P < 0.001$) after 3 weeks of induction (Fig. 4B).

Cartilage-like cells within lacunae and a large amount of cartilage extracellular matrix were observed in sections of pellets from

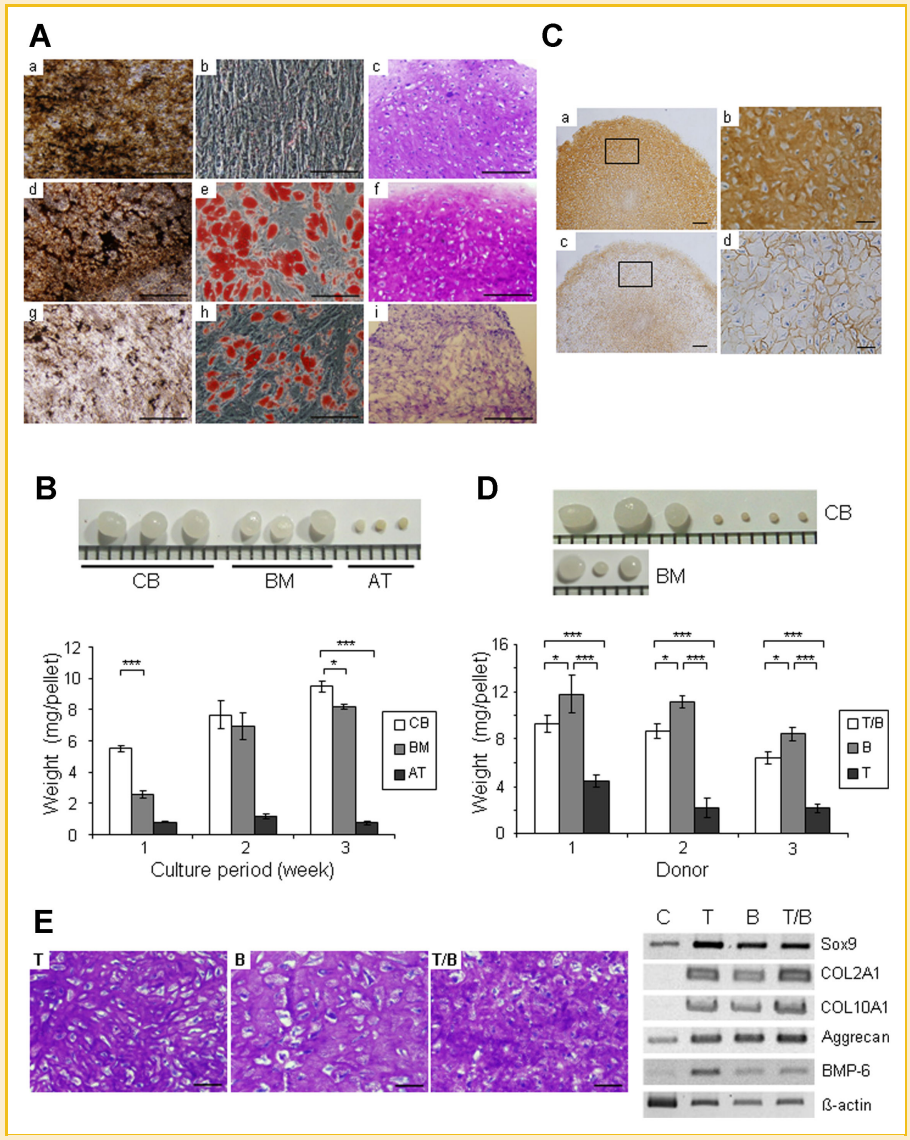

Fig. 4. Differentiation capability of CB-MSC, BM-MSC, and AT-MSC. A: Multilineage differentiation of CB-MSC, BM-MSC, and AT-MSC. Osteogenic differentiation demonstrated by deposition of mineralized matrix detected by von Kossa staining. CB-MSC (a), BM-MSC (d), and AT-MSC (g) were positive. Adipogenic differentiation demonstrated by accumulation of lipid vacuoles indicated by Oil Red O staining. Most CB-MSC (b) were negative for Oil Red O staining. BM-MSC (e), and AT-MSC (h) were positive. Chondrogenic differentiation demonstrated by toluidine blue staining (proteoglycan extracellular matrix staining) of paraffin sections of cell pellets induced by TGF-β3 plus BMP-2 for 3 weeks. The pellets of CB-MSC (c) and BM-MSC (f) showed cartilage-like cells within lacunae, and a large amount of cartilage extracellular matrix were stained strongly with toluidine blue. In contrast, there were no significant cartilage-like cells and very little extracellular matrix was stained by toluidine blue in the pellet of AT-MSC (i). Scale bars: 200 μm. B: Chondrogenic differentiation of CB-MSC, BM-MSC, and AT-MSC. Top: Chondrocyte pellets of CB-MSC, BM-MSC, and AT-MSC from three different donors cultured for 3 weeks. The pellets of CB-MSC and BM-MSC were white with some transparency and bigger than AT-MSC pellets. Scale ruler: 1 mm. Bottom: Average weight of pellets of CB-MSC ($n = 10$), BM-MSC ($n = 6$), and AT-MSC ($n = 10$) during 3-week induction by TGF-β3 plus BMP-2. C: Immunohistologic staining of CB-MSC pellet. Staining of the extracellular matrix with anti-type II collagen (a,b). Staining with anti-type I collagen (c,d). The extracellular matrix was not stained with anti-type I collagen, however, surface layers of the pellets were faintly positive. Scale bars: 200 μm (a,c), scale bars: 50 μm (b,d). D: Effect of cytokines on chondrogenesis of MSC in vitro for 3 weeks. Top: First row; pellets ($n = 6$) from CB-MSC induced with (left to right): TGF-β3 plus BMP-2, BMP-2, TGF-β3, insulin, IGF-1, FGF-2, no cytokines. Second row; pellets of BM-MSC induced with (left to right): TGF-β3 plus BMP-2, BMP-2 alone and TGF-β3. Scale ruler: 1 mm. Bottom: Average weight of pellets (mg/pellet) of three CB-MSC cultured with: TGF-β3 and BMP-2 (T/B), BMP-2 (B), and TGF-β3 (T) for 21 days. Pellets from cultures treated with BMP-2 or BMP-2 and TGF-β3 were consistently heavier than those treated with TGF-β3 alone ($P < 0.001$). Furthermore, the pellets treated with BMP-2 alone were heavier than those treated with BMP-2 and TGF-β3 ($P < 0.05$). E: Effect of TGF-β3 and BMP-2 on the structure of CB-MSC pellets and chondrogenic gene expression. Left: Histological staining of the pellets cultured with TGF-β3 and/or BMP-2 for 21 days. In the central area of the pellets, abundant metachromatic matrix was formed, and many hypertrophic chondrocytes appeared in the pellets induced by BMP-2 alone. Sections of the pellets were stained with toluidine blue. Scale bars: 50 μm. Right: Expression of chondrogenesis-related genes detected by RT-PCR after 21 days of culture ($n = 3$). (T) induced with TGF-β3, (B) induced with BMP-2, (T/B) induced with TGF-β3 plus BMP-2, (C) uninduced control of CB-MSC. $^{*}P < 0.05$ $^{***}P < 0.001$.

CB-MSC and BM-MSC stained with toluidine blue, but not in sections of pellets from AT-MSC (Fig. 4A). Type II collagen was strongly stained in the extracellular matrix of CB-MSC, but type I collagen was not (Fig. 4C).

Insulin, IGF-1, and FGF-2 produced no effect on the growth of the pellet (Fig. 4D). The pellets induced by TGF-β3 were smaller, and the pellets induced by BMP-2 were larger than those induced by the combination of TGF-β3 and BMP-2. Histological and expression analysis of chondrocyte-related genes confirmed that chondrogenic differentiation of CB-MSC was induced by TGF-β3, BMP-2, and their combination (Fig. 4E). However, many hypertrophic chondrocytes were observed in the pellets induced by BMP-2 in the absence of TGF-β3.

In examination of long-term cultures, the size and weight of pellets of CB-MSC cultured with TGF-β3 plus BMP-2 was found to increase continuously up to 6 weeks (Fig. S8).

All BM-MSC (6/6) and AT-MSC (21/21), but only 8.9% of CB-MSC (4/45) showed adipogenic differentiation (Fig. 4A). In the four CB-MSC samples that exhibited adipogenic differentiation, smaller oil droplets were formed within the cells, and the frequency of positive cells was much lower than in BM-MSC or AT-MSC (data not shown).

CHONDROGENESIS AND OSTEOGENESIS OF CB-MSC IN VIVO

By the third week following subcutaneous transplantation of the collagen sponge with CB-MSC, the construct had changed glistening, white, stiff tissue resembling cartilage (Fig. 5A). Cartilage-like cells were observed within lacunae, and a large amount of cartilage extracellular matrix stained with toluidine blue and type II collagen were formed around collagen fibers. No blood vessel formation was observed in the composite. By the 8 weeks following subcutaneous transplantation of the construct of CB-MSC and β-TCP, decalcified sections stained with hematoxylin and eosin exhibited a large quantity of bone tissue formation in multiple pores of β-TCP (Fig. 5B).

GENE EXPRESSION IN CB-MSC, BM-MSC, AND AT-MSC

The expression patterns of stem cell markers in CB-MSC were similar to those of BM-MSC and AT-MSC (Fig. 6A). In addition, the osteoblast transcription factor, Cbfa1, adipocyte transcription factors, PPAR-γ1 and PPAR-γ2, BMP-receptors (BMPR-IA, -IB, and -II), intracellular effectors of BMP signal, Smad1, 5, and 8 were detected in all MSC. The expression of Sox5, Sox6, and Sox9 were stronger in CB-MSC than in BM-MSC or AT-MSC.

EXPRESSION OF DLK-1 AND ADIPOCYTE DIFFERENTIATION

The DLK-1 gene was expressed in half of CB-MSC cell lines (7/15, 47%, passage <5; Fig. 6B). Expression of DLK-1 was the same in single cell clones as it was in the parental cell lines (data not shown). Two of seven DLK-1 positive cell lines exhibited expression of DLK-1 that was about 100 times higher than the other lines (Fig. 6C). There was no correlation between DLK-1 expression and adipocytic differentiation ability (Fig. 6B).

IMMUNOSUPPRESSIVE EFFECT OF CB-MSC

CB-MSC suppressed proliferation of phytohemagglutinin (PHA) (Sigma–Aldrich) and alloantigen stimulated T-cells in a cell dose dependent manner (Fig. 7A). CB-MSC were as effective as BM-MSC and AT-MSC in suppressing proliferation of PHA stimulated lymphocytes (Fig. 7B).

DISCUSSION

Although many reports of CB-MSC have been published over the last 10 years, controversy still exists as to whether CB can serve as a good cell source of MSC for cell therapy or regenerative medicine [Flynn et al., 2007; Secco et al., 2008; Harris, 2009; Fong et al., 2010]. This controversy is derived in part from the difficulty of isolating CB-MSC consistently. Even though most of the groups have adopted recommended conditions from the literature to maximize recovery of CB-MSC, including selecting full-term CB units, allowing a storage time of less than 15 h, ensuring a cord volume of more than 33 ml, and a MNC count greater than 1×10^8 as the selection criteria for CB units [Bieback et al., 2004], yields have varied widely, from fewer than 10% to as high as 60% [Secco et al., 2008; Avanzini et al., 2009; Fong et al., 2010; Morigi et al., 2010; Zeddou et al., 2010].

In this study we achieved a high rate of success in isolation of CB-MSC of 90%, when CB volume was $\geq$90 ml and the interval time was $\leq$2 h (Fig. 2C). We found no benefit from using protein-coated plates [Bieback et al., 2004; Maurice et al., 2007], depletion of lymphocytes and monocytes from MNC before plating [Lee et al., 2004; Avanzini et al., 2009], culturing cells in hypoxic conditions [Dos Santos et al., 2010], or addition of cytokines (SCF, IL-3 plus FGF-2) to the primary culture medium [Fan et al., 2009]. We observed that colony-forming cells disappeared or lost their colony-forming ability within 2 h after collection although in about half of the cord blood units a small number of CB-MSC cells could be successfully propagated even after longer periods of time. The time dependence of CB-MSC recovery admirably fitted the equation of KJMA model commonly used to explain nucleation [Ben-Naim and Krapivsky, 1996] and mortality processes [Williams et al., 1992; Hirsh et al., 1994]. However, the time exponent in this particular model is considerably less than 1.0 which implies that the mechanism(s) causing the loss of cells are themselves disappearing with time. The exact biological mechanism for this slowing rate of decline of successful isolations with time is not presently resolved. Possible mechanisms to be tested include physical changes in the cells, such as time dependent changes in cell density due to exposure to the functionally hypotonic anticoagulant solution, adhesion to plastic surfaces in the collection container and biological changes due to exposure to normoxia. Further experiments are planned to characterize and mitigate this phenomenon of reduced recovery over time.

A second objective of the present research was to characterize the biology of CB-MSC using BM-MSC and AT-MSC as reference controls. The first observation we made was that the kinetics of CB-MSC proliferation are substantially higher than either AT-MSC or BM-MSC (Fig. 1B). For clinical studies, it is often desirable to have a cell dose on the order of 1×10^9 cells [Osiris Ther, Inc. Clinical Trials, http://www.osiris.com/clinical.php]. We found that 1.65×10^6 of CB-MSC obtained from a single cord blood unit was sufficient to

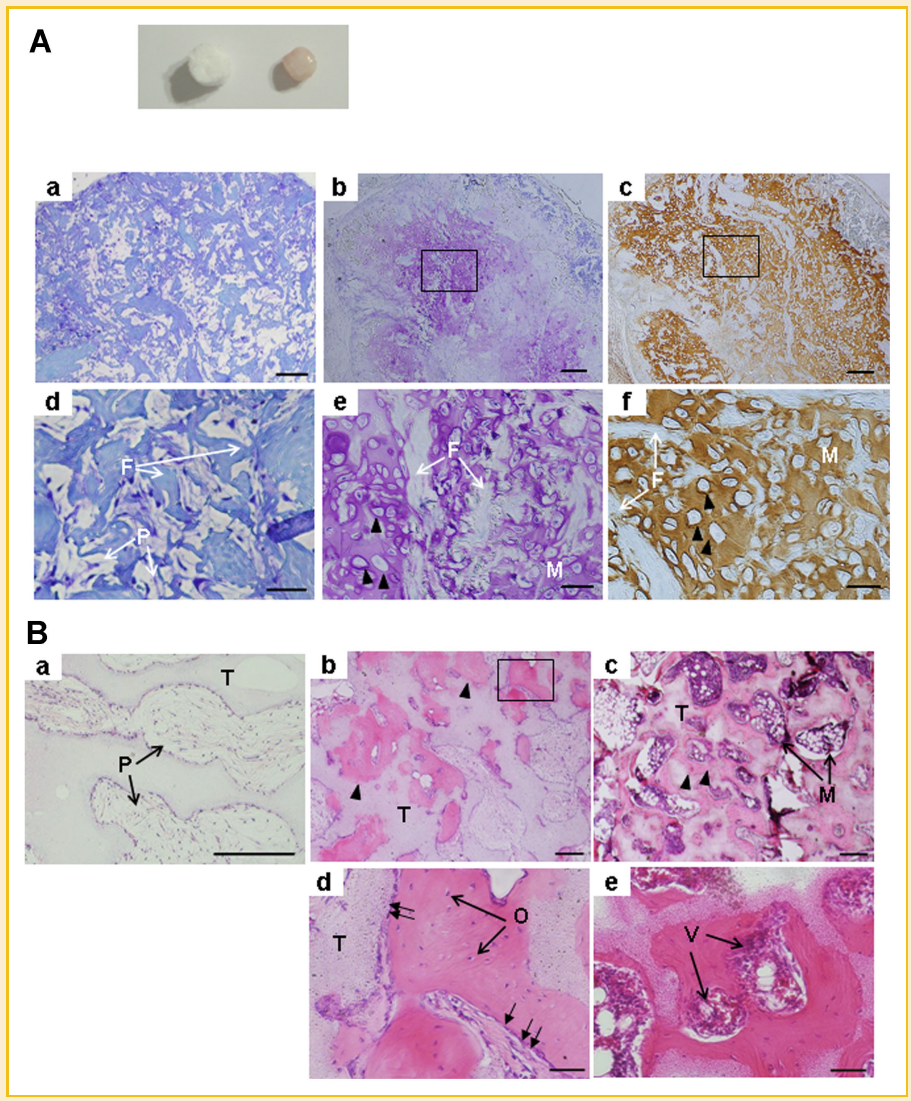

Fig. 5. Chondrogenesis and osteogenesis of CB-MSC in vivo. A: In vivo chondrogenesis of CB-MSC in collagen sponge. CB-MSC were loaded into a collagen sponge and cultured in vitro for 2 weeks in chondrogenic medium. Cultured sponges were implanted into subcutaneous pockets in nude mice for another 3 weeks. Top-left: Collagen sponge without cells (5 mm in diameter by 3 mm in thickness), (top-right) composite of CB-MSC and collagen sponge 3 weeks after implantation. Bottom: At 2 weeks of in vitro culture, cells filled the pores of collagen sponges, and a portion of extracellular matrix was stained with toluidine blue (a,d). Cartilage-like cells within lacunae and a large amount of cartilage extracellular matrix were formed between the collagen fibers, which were positive to toluidine blue (b,e). Type II collagen staining (c,f). No blood vessel formation was observed in the composite. F, fibers of collagen; arrowhead, chondrocytes; M, extracellular matrix; P, pore of sponge. a,b,c: Scale bars: 200 μm. d,e,f: Scale bars: 50 μm. B: Osteogenesis of CB-MSC in vivo. CB-MSC loaded into a β-TCP scaffold were cultured in the osteogenic induction medium for 2 weeks and then transplanted under the skin of nude mice for 8 weeks. Control β-TCP scaffold (T) without CB-MSC 8 weeks after transplantation (a). Large amount of newly bone was formed in the pores of implanted scaffold with CB-MSC (b,c). On the periphery of β-TCP scaffold osteoblasts (arrows) and osteocytes were observed (d). Mature bone with bone marrow-like tissue and thick layers of lamellar bone and blood vessels were formed in the composite (c,e). O, osteocytes; M, mature bone; V, vessels; P, pore of β-TCP. a,b,c: Scale bars: 200 μm, (d,e) Scale bars: 50 μm. Sections were stained with hematoxylin and eosin.

generate 1×10^9 CB-MSC within 3–4 passages using multilayer flasks (Fig. 3C). However, the size of the chondrocyte pellet obtained after large scale expansion of CB-MSC was smaller than the chondrocyte pellet obtained before expansion in the culture chamber (Fig. 3D). Therefore, one important objective will be the development of new devices for large scale cell expansion with better conditions for MSC.

After extensive tissue culture expansion, an important safety issue is karyotype stability. There are conflicting reports on the stability of chromosomes in BM-MSC cultured for long periods with evidence of possible transformation due to by the contaminating tumor cells rather than derived from the MSC [Prockop et al., 2010]. The stability of CB-MSC was detected by Avanzini et al. [2009] by molecular karyotyping. In this study, we found that expanded CB-MSC retained high karyotypic stability after 8–20 passages (Fig. 3E). Recently Tarte et al. reported the occurrence of aneuploidy in BM-MSC at early passages, but the cells did not exhibit any transforming events. They concluded that the aneuploidy was not related to the

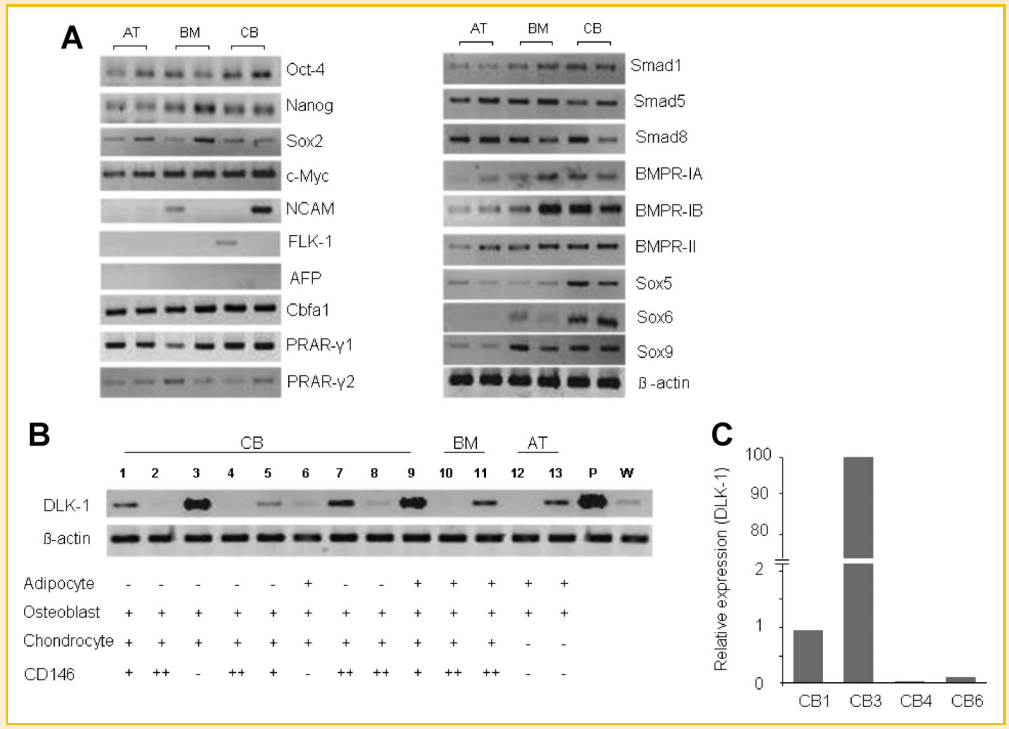

Fig. 6. Gene expression in CB-MSC, BM-MSC, and AT-MSC. A: Gene expression in two typical cells lines of CB-MSC (10 tested), BM-MSC (6 tested) and AT-MSC (5 tested) by RT-PCR. B: DLK-1 expression in CB-MSC and ability to differentiate to adipocyte, osteoblast, and chondrocyte. CD146 expression was obtained by flow cytometry as in Figure 3B. P: positive control (Total RNA from human fetal liver, Clontech). W: WI38 (normal human fetal lung fibroblasts, ATCC) served as negative control. Results from 9 CB-MSC (ex utero collection), 2 BM-MSC, and 2 AT-MSC samples are shown. CD146 expression indicated as range of percent positive cells: −, 0–5%; +, 5–60%; ++, 60–100%. We found 7 CB units DLK-1 positive (volume of CB, 69.3 ± 18.8 ml, time 1.4 ± 0.6 h) and 8 CB units DLK-1 negative (volume of CB, 63.3 ± 10.5 ml, time 1.6 ± 0.5 h). Regarding CD146 marker, the results are as follow: CD146 ++ CB-MSC (volume, 68.8 ± 13.1 ml, time 1.6 ± 0.3 h, n = 10), CD146 + CB-MSC (volume, 54.7 ± 9.4 ml, time 1.1 ± 0.4 h, n = 7), and CD146 − CB-MSC (volume, 81.6 ± 17.1 ml, time 2.0 ± 0.5 h, n = 3). C: DLK-1 expression in CB-MSC measured by quantitative RT-PCR. Signals were normalized to the highest signal (CB3) which was set to 100%. Results of 4 CB-MSC cell lines are shown. The CB1, CB3, CB4, and CB6 shown in (C) match with the CB units shown in (B).

culture process but could have been donor dependent [Tarte et al., 2010]. These data suggest that the quality of the established CB-MSC lines in our study was equivalent to the quality of BM-MSC [Prockop et al., 2010; Tarte et al., 2010]. Selection of stable cell lines and careful evaluation by molecular karyotyping would be important in therapeutic applications of CB-MSC.

MSC have a well described immunomodulatory effect [Nauta and Fibbe, 2007] that has been used to treat refractory severe aGVHD

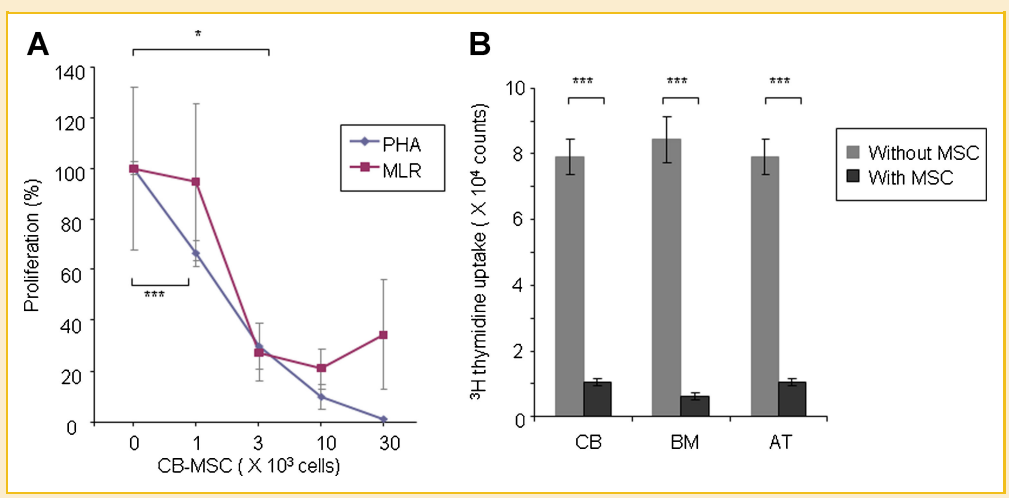

Fig. 7. Suppressive effect of MSC on proliferation of activated peripheral T lymphocytes. A: Dose dependent inhibitory effect of CB-MSC on proliferation of alloantigen and PHA stimulated T lymphocytes. B: Inhibitory effect of CB-MSC, BM-MSC, and AT-MSC on proliferation of PHA stimulated T cell. $^{*}P < 0.05$, $^{***}P < 0.001$. [Color figure can be viewed in the online issue, which is available at wileyonlinelibrary.com.]

[Prasad et al., 2010]. In our comparative study, CB-MSC showed immunomodulation activity that was equivalent to BM-MSC and AT-MSC as reported previously [Avanzini et al., 2009; Wang et al., 2009] (Fig. 7).

Previous reports have indicated that CB-MSC have the potential to be differentiated to various cell types such as chondrocytes, osteocytes, cardiomyocytes, and pancreatic cells and have the functional potential to repair acute kidney injury, to support hematopoietic stem cell expansion as feeder cells, and to possess immunosuppressive activities [Nishiyama et al., 2007; Reinisch et al., 2007; Avanzini et al., 2009; Morigi et al., 2010]. Among these qualities, the high capacity to differentiate into chondrocytes would appear to represent an advantage among various tissue-derived MSC. The expression of BMP receptors was detected in CB-MSC and BM-MSC (Fig. 6A). The different responses of CB-MSC and BM-MSC to BMP-2 might be related to the alteration of extracellular signaling pathway by aging [Moerman et al., 2004]. Higher gene expression of Sox family may support the higher chondrogenesis ability of CB-MSC.

Unlike BM-MSC and AT-MSC, CB-MSC showed a relatively low ability to differentiate toward the adipocyte lineage, as was previously reported [Yu et al., 2004; Kern et al., 2006; Morigi et al., 2010], despite expression of PPAR-γ gene, which is essential for adipocyte formation. Low differentiation adipocyte ability was also observed in placental microvilli derived MSC in our previous study [Igura et al., 2004]. DLK-1 is a pre-adipocyte factor, and was proposed to be a specific marker for USSC [Kluth et al., 2010]. In our study, the CB-MSC cell lines with low or no adipocytic differentiation ability did not express DLK-1, and there was no correlation found between either DLK-1 expression and adipocyte differentiation ability or between DLK-1 and CD146 expression (Fig. 6B). Further study is necessary to elucidate the meaning of DLK-1 and CD 146 expression, and to define the differences and similarities between CB-MSC and USSC.

The origin of MSC in CB is not known but there is a possibility that the cells are released from fetal liver or fetal bone marrow into the fetal circulation. Recently, perivascular cells, including pericytes, have been proposed as the origin of MSC in various tissues [Covas et al., 2008; Corselli et al., 2010]. We detected one of the typical surface markers of pericytes, CD146, on our CB-MSC although its expression was highly variable (range from 3.5% to 98.4%; Fig. 3B). The variable expression of CD146 contrasted with expression of all other MSC cell surface markers, the expression of which was consistent regardless of cord blood unit from which they were derived. In contrast, CD146 was expressed at 65–90% level in BM-MSC, and only at a trace level in AT-MSC. CD146 has been proposed as a marker of multipotency; a twofold difference in expression has been shown between unipotent and tripotent clones in BM-MSC [Russell et al., 2010]. We did not find any correlation between CD146 expression and differentiation ability of CB-MSC samples (Fig. 6B). Further study is necessary to elucidate the origin of CB-MSC and the significance of different expression levels of CD146.

In summary, we have identified a reliable means for establishing CB-MSC lines from freshly donated cord blood units. Further, we have demonstrated that CB-MSC exhibit a significantly different biological profile when directly compared with BM-MSC and AT-MSC.

Although MSC can be isolated from many tissues, CB may be a preferred source of MSC for applications in regenerative medicine and cell therapy.

ACKNOWLEDGMENTS

We thank all of the mothers who allowed us to use the cord blood, and the collection facilities of the National Cord Blood Program and Yamaguchi Hospital for their kind collaboration on collecting cord blood. We thank Dr. G. Vunjak-Novakovic, Biomedical Engineering Department, Columbia University, for her critical reading and advice on the manuscript. This work was partially supported by Research Grant 364 on Human Genome, Tissue Engineering from The Japanese Ministry of Health, Labor and Welfare; Contract grant number: HP-D14, H17365022.

REFERENCES

Avanzini MA, Bernardo ME, Cometa AM, Perotti C, Zaffaroni N, Novara F, Visai L, Moretta A, Del Fante C, Villa R, Ball LM, Fibbe WE, Maccario R, Locatelli F. 2009. Generation of mesenchymal stromal cells in the presence of platelet lysate: A phenotypic and functional comparison of umbilical cord blood- and bone marrow-derived progenitors. Haematologica 94:1649–1660.

Ben-Naim E, Krapivsky PL. 1996. Nucleation and growth in one dimension. Phys Rev E Stat Phys Plasmas Fluids Relat Interdiscipl Top 54:3562–3568.

Bieback K, Kern S, Kluter H, Eichler H. 2004. Critical parameters for the isolation of mesenchymal stem cells from umbilical cord blood. Stem Cells 22:625–634.

Caplan AI. 2007. Adult mesenchymal stem cells for tissue engineering versus regenerative medicine. J Cell Physiol 213:341–347.

Corselli M, Chen CW, Crisan M, Lazzari L, Peault B. 2010. Perivascular ancestors of adult multipotent stem cells. Arterioscler Thromb Vasc Biol 30: 1104–1109.

Covas DT, Panepucci RA, Fontes AM, Silva WA, Jr., Orellana MD, Freitas MC, Neder L, Santos AR, Peres LC, Jamur MC, Zago MA. 2008. Multipotent mesenchymal stromal cells obtained from diverse human tissues share functional properties and gene-expression profile with CD146+ perivascular cells and fibroblasts. Exp Hematol 36:642–654.

Dos Santos F, Andrade PZ, Boura JS, Abecasis MM, da Silva CL, Cabral JM. 2010. Ex vivo expansion of human mesenchymal stem cells: A more effective cell proliferation kinetics and metabolism under hypoxia. J Cell Physiol 223:27–35.

Erices A, Conget P, Minguell JJ. 2000. Mesenchymal progenitor cells in human umbilical cord blood. Br J Haematol 109:235–242.

Fan X, Liu T, Liu Y, Ma X, Cui Z. 2009. Optimization of primary culture condition for mesenchymal stem cell derived from umbilical cord blood with factorial design. Biotechnol Prog 25:499–507.

Flynn A, Barry F, O'Brien T. 2007. UC blood-derived mesenchymal stromal cells: An overview. Cytotherapy 9:718–726.

Fong CY, Subramanian A, Biswas A, Gauthaman K, Srikanth P, Hande MP, Bongso A. 2010. Derivation efficiency, cell proliferation, freeze-thaw survival, stem-cell properties and differentiation of human Wharton's jelly stem cells. Reprod Biomed Online 21:391–401.

Garcia J. 2010. Allogeneic unrelated cord blood banking worldwide: An update. Transfus Apher Sci 42:257–263.

Harris DT. 2009. Non-haematological uses of cord blood stem cells. Br J Haematol 147:177–184.

Hirsh AG, Williams RJ, Mehl P. 1994. Kinetics of medfly mortality. Exp Gerontol 29:197–204.

Igura K, Zhang X, Takahashi K, Mitsuru S, Yamaguchi S, Takahashi TA. 2004. Isolation and characterization of mesenchymal progenitor cells from chorionic villi of human placenta. Cytotherapy 6:543–553.

Kern S, Eichler H, Stoeve J, Kluter H, Bieback K. 2006. Comparative analysis of mesenchymal stem cells from bone marrow, umbilical cord blood, or adipose tissue. Stem Cells 24:1294–1301.

Kluth SM, Buchheiser A, Houben AP, Geyh S, Krenz T, Radke TF, Wiek C, Hanenberg H, Reinecke P, Wernet P, Kögler G. 2010. DLK-1 as a marker to distinguish unrestricted somatic stem cells and mesenchymal stromal cells in cord blood. Stem Cells Dev 19:1471–1483.

Kögler G, Sensken S, Airey JA, Trapp T, Müschen M, Feldhahn N, Liedtke S, Sorg RV, Fischer J, Rosenbaum C, Greschat S, Knipper A, Bender J, Degistirici O, Gao J, Caplan AI, Colletti EJ, Almeida-Porada G, Müller HW, Zanjani E, Wernet P. 2004. A new human somatic stem cell from placental cord blood with intrinsic pluripotent differentiation potential. J Exp Med 200:123–135.

Kögler G, Radke TF, Lefort A, Sensken S, Fischer J, Sorg RV, Wernet P. 2005. Cytokine production and hematopoiesis supporting activity of cord blood-derived unrestricted somatic stem cells. Exp Hematol 33:573–583.

Le Blanc K, Frassoni F, Ball L, Locatelli F, Roelofs H, Lewis I, Lanino E, Sundberg B, Bernardo ME, Remberger M, Dini G, Egeler RM, Bacigalupo A, Fibbe W, Ringdén O, Developmental Committee of the European Group for Blood and Marrow Transplantation. 2008. Mesenchymal stem cells for treatment of steroid-resistant, severe, acute graft-versus-host disease: A phase II study. Lancet 371:1579–1586.

Lee OK, Kuo TK, Chen WM, Lee KD, Hsieh SL, Chen TH. 2004. Isolation of multipotent mesenchymal stem cells from umbilical cord. Blood 103:1669–1675.

Maurice S, Srouji S, Livne E. 2007. Isolation of progenitor cells from cord blood using adhesion matrices. Cytotechnology 54:121–133.

Moerman EJ, Teng K, Lipschitz DA, Lecka-Czernik B. 2004. Aging activates adipogenic and suppresses osteogenic programs in mesenchymal marrow stroma/stem cells: The role of PPAR-gamma2 transcription factor and TGF-beta/BMP signaling pathways. Aging Cell 3:379–389.

Morigi M, Rota C, Montemurro T, Montelatici E, Lo Cicero V, Imberti B, Abbate M, Zoja C, Cassis P, Longaretti L, Rebulla P, Introna M, Capelli C, Benigni A, Remuzzi G, Lazzari L. 2010. Life-sparing effect of human cord blood-mesenchymal stem cells in experimental acute kidney injury. Stem Cells 28:513–522.

Nauta AJ, Fibbe WE. 2007. Immunomodulatory properties of mesenchymal stromal cells. Blood 110:3499–3506.

Nishiyama N, Miyoshi S, Hida N, Uyama T, Okamoto K, Ikegami Y, Miyado K, Segawa K, Terai M, Sakamoto M, Ogawa S, Umezawa A. 2007. The significant cardiomyogenic potential of human umbilical cord blood-derived mesenchymal stem cells in vitro. Stem Cells 25:2017–2024.

Parolini O, Alviano F, Bagnara GP, Bilic G, Bühring HJ, Evangelista M, Hennerbichler S, Liu B, Magatti M, Mao N, Miki T, Marongiu F, Nakajima H, Nikaido T, Portmann-Lanz CB, Sankar V, Soncini M, Stadler G, Surbek D, Takahashi TA, Redl H, Sakuragawa N, Wolbank S, Zeisberger S, Zisch A, Strom SC. 2008. Concise review: Isolation and characterization of cells from human term placenta: Outcome of the first international workshop on placenta derived stem cells. Stem Cells 26:300–311.

Pittenger MF, Mackay AM, Beck SC, Jaiswal RK, Douglas R, Mosca JD, Moorman MA, Simonetti DW, Craig S, Marshak DR. 1999. Multilineage potential of adult human mesenchymal stem cells. Science 284:143–147.

Prasad VK, Lucas KG, Kleiner GI, Talano JA, Jacobsohn D, Broadwater G, Monroy R, Kurtzberg J. 2010. Efficacy and safety of ex-vivo cultured adult human mesenchymal stem cells (Prochymal™) in pediatric patients with severe refractory acute graft-versus-host disease in a compassionate use study. Biol Blood Marrow Transplant DOI: 10.1016/j.bbmt.2010.04.014.

Prockop DJ. 2009. Repair of tissues by adult stem/progenitor cells (MSCs): Controversies, myths, and changing paradigms. Mol Ther 17:838–946.

Prockop DJ, Brenner M, Fibbe WE, Horwitz E, Le Blanc K, Phinney DG, Simmons PJ, Sensebe L, Keating A. 2010. Defining the risks of mesenchymal stromal cell therapy. Cytotherapy 12:576–578.

Reinisch A, Bartmann C, Rohde E, Schallmoser K, Bjelic-Radisic V, Lanzer G, Linkesch W, Strunk D. 2007. Humanized system to propagate cord blood-derived multipotent mesenchymal stromal cells for clinical application. Regen Med 2:371–382.

Rubinstein P. 2009. Cord blood banking for clinical transplantation. Bone Marrow Transplant 44:635–642.

Rubinstein P, Dobrila L, Rosenfield RE, Adamson JW, Migliaccio G, Migliaccio AR, Taylor PE, Stevens CE. 1995. Processing and cryopreservation of placental/umbilical cord blood for unrelated bone marrow reconstitution. Proc Natl Acad Sci USA 92:10119–10122.

Russell KC, Phinney DG, Lacey MR, Barrilleaux BL, Meyertholen KE, O'Connor KC. 2010. In vitro high-capacity assay to quantify the clonal heterogeneity in trilineage potential of mesenchymal stem cells reveals a complex hierarchy of lineage commitment. Stem Cells 28:788–798.

Salem HJ, Thiemermann C. 2010. Mesenchymal stromal cells: Current understanding and clinical status. Stem Cells 28:585–596.

Sarugaser R, Lickorish D, Baksh D, Hosseini MM, Davies JE. 2005. Human umbilical cord perivascular (HUCPV) cells: A source of mesenchymal progenitors. Stem Cells 23:220–229.

Secco M, Zucconi E, Vieira NM, Fogaça LL, Cerqueira A, Carvalho MD, Jazedje T, Okamoto OK, Muotri AR, Zatz M. 2008. Multipotent stem cells from umbilical cord: Cord is richer than blood! Stem Cells 26:146–150.

Sul HS. 2009. Minireview: Pref-1: Role in adipogenesis and mesenchymal cell fate. Mol Endocrinol 23:1717–1725.

Tarte K, Gaillard J, Lataillade JJ, Fouillard L, Becker M, Mossafa H, Tchirkov A, Rouard H, Henry C, Splingard M, Dulong J, Monnier D, Gourmelon P, Gorin NC, Sensebé L, Société Française de Greffe de Moelle et Thérapie Cellulaire. 2010. Clinical-grade production of human mesenchymal stromal cells: Occurrence of aneuploidy without transformation. Blood 115:1549–1553.

Troyer DL, Weiss ML. 2008. Wharton's jelly-derived cells are a primitive stromal cell population. Stem Cells 26:591–599.

Wagner JE, Gluckman E. 2010. Umbilical cord blood transplantation: The first 20 years. Semin Hematol 47:3–12.

Wang M, Yang Y, Yang D, Luo F, Liang W, Guo S, Xu J. 2009. The immunomodulatory activity of human umbilical cord blood-derived mesenchymal stem cells in vitro. Immunology 126:220–232.

Williams RJ, Takahashi T, Hirsh AG. 1992. The kinetics of autolysis in osmotically stressed sea urchin eggs. Thermochimica Acta 203:493–501.

Ye ZQ, Burkholder JK, Qiu P, Schultz JC, Shahidi NT, Yang NS. 1994. Establishment of an adherent cell feeder layer from human umbilical cord blood for support of long-term hematopoietic progenitor cell growth. Proc Natl Acad Sci USA 91:12140–12144.

Yu M, Xiao Z, Shen L, Li L. 2004. Mid-trimester fetal blood-derived adherent cells share characteristics similar to mesenchymal stem cells but full-term umbilical cord blood does not. Br J Haematol 124:666–675.

Zeddou M, Briquet A, Relic B, Josse C, Malaise MG, Gothot A, Lechanteur C, Beguin Y. 2010. The umbilical cord matrix is a better source of mesenchymal stem cells (MSC) than the umbilical cord blood. Cell Biol Int 34:693–701.

Zhang X, Mitsuru A, Igura K, Takahashi K, Ichinose S, Yamaguchi S, Takahashi TA. 2006. Mesenchymal progenitor cells derived from chorionic villi of human placenta for cartilage tissue engineering. Biochem Biophys Res Commun 340:944–952.